LAWRENCE
LIVERMORE
NATIONAL
LABORATORY

UCRL-TR-224124

Crustal Structure of Iraq from Receiver Functions and Surface Wave Dispersion

R. Gok, H. Mahdi, H. Al-Shukri, A. J. Rodgers

August 31, 2006

This work was performed under the auspices of the U.S. Department of Energy by University of California, Lawrence Livermore National Laboratory under Contract W-7405-Eng-48.

Crustal Structure of Iraq from Receiver Functions and Surface Wave Dispersion

Rengin Gök[1], Hanan Mahdi[2], Haydar Al-Shukri[2], and Arthur J. Rodgers[1]

[1] Energy and Environment Directorate, Lawrence Livermore National Laboratory Livermore, CA
[2] Applied Science Department, University of Arkansas at Little Rock, Little Rock, AR

Abstract

We report the crustal structure of Iraq, located in the northeastern Arabian plate, estimated by joint inversion of P-wave receiver functions and surface wave group velocity dispersion. Receiver functions were computed from teleseismic recordings at two temporary broadband seismic stations in Mosul (MSL) and Baghdad (BHD), separated by approximately 360 km. Group velocity dispersion curves at the sites were derived from continental-scale tomography of Pasyanos (2006). The inversion results show that the crustal thicknesses are 39 km at MSL and 43 km at BHD. Both sites reveal low velocity surface layers consistent with sedimentary thickness of about 3 km at station MSL and 7 km at BHD, agreeing well with the existing models. Ignoring the sediments, the crustal velocities and thicknesses are remarkably similar between the two stations, suggesting that the crustal structure of the proto-Arabian Platform in northern Iraq was uniform before subsidence and deposition of the sediments in the Cenozoic. Deeper low velocity sediments at BHD are expected to result in higher ground motions for earthquakes.

Introduction

Iraq is located in the northern Arabian Platform including the western edge of the Zagros Mountain range, where the convergent tectonic boundary between the Eurasian and Arabian plates forms a fold and thrust belt. Tectonics and geology of Iraq have been influenced by the proximity of the Pre-Cambrian Arabian Shield to the southwest and the Zagros Province of the Tethyan geosyncline to the east (Al-Naqib, 1967). The high Bitlis-Zagros Mountains in the north and eastern part of the country are a folded belt in a

NW-SE direction along the western part of Iran and northeast Iraq. They extend from Oman in the southeast to the Turkish border in the northwest (Adams and Barazangi, 1984). The folding probably started during the Upper Miocene-Lower Pliocene, and the belt is still considered to be one of the most active orogens on earth (Stocklin, 1968; Kassler, 1973). Iraq can be divided into three tectonic zones: the unfolded (stable platform), folded, and the thrust zones (Figure 1). These units were differentiated during the late Tertiary (mainly Pliocene) Alpine orogeny (Dunnington, 1958). The Mesopotamian foredeep covers an intermediate structural position between the Alpine geosynclinal area of Zagros in N-NE part of Iraq and the Pre-Cambrian African-Arabian platform to the west. This zone is characterized by a great subsidence since Mesozoic time until late Cenozoic with slight folding of sedimentary cover up to 9 km (Laske et al., 1997; Seber et al., 1997). The third zone is the northern part of African-Arabian Pre-Cambrian platform and is characterized by unfolded stable zone, an almost horizontal dipping strata and smooth relief (Ditmar et.al., 1971).

Earthquakes in the Zagros Fold and Thrust define a zone of approximately 200 km width, which runs parallel to the folded belt (Nowroozi, 1972; Berberian, 1976; Kadinsky-Cade and Barazangi, 1982). The majority of the moderate-to-large historical events in eastern Iraq have occurred along this belt (Alsinawi and Ghalib, 1975; Alsinawi and Banno, 1976; Alsinawi and A1-Shukri, 1979). In general, seismicity in the Zagros Mountains of Iraq has intermediate to shallow focus seismicity with focal depths ranging from 30-50 km (Engdahl et al., 1998; Engdahl et al., 2006).

Tomographic images of seismic structure of the Middle East have been estimated from Pn travel time tomography (Hearn and Ni, 1994; Al-Lazki et al., 2003, 2004), surface wave group velocity dispersion (e.g. Ritzwoller and Levshin, 1998; Pasyanos, 2005) and partitioned waveform inversion (Maggi and Priestley, 2005). These studies report faster mantle velocities beneath the Arabian Platform and slower velocities beneath the Turkish-Iranian Plateau. Estimates of crustal structure in the northern Arabian Platform are limited due to the paucity of active and passive seismic investigations. The exceptions are Kuwait and southeastern Turkey. For Kuwait,

Pasyanos et al. (in preparation) report crustal thickness of 45 km with 8 km of sedimentary cover. Using the spectral ratio method on digitized records Al-Heety, 2006 found that the crustal thickness is 38 km at BHD station. For southeastern Turkey, Gök et al. (2006) reported a crustal thickness of 38 km with 2 km of sediments. A crustal profile from the northern Arabian/Persian Gulf across the Zagros Mountains to the Iranian Plateau by Paul et al. (2006) found crustal thickness of 45 west of the MZT (Main Zagros Thrust) with significant thickening (~70 km) east of MZT. Al-Damegh et al., (2004) demonstrated short-period regional wave propagation complexity of the region using Lg and Sn propagation efficiencies. They found that the Arabian plate had efficient Lg propagation but the seismically active regions in Iran and Turkey had Lg blockage. In particular there is a sharp boundary between the Sn and Lg propagation at the region between Arabian Plate and Bitlis/Zagros suture in Iran-Iraq border (Gök et al., 2003; Al-Damegh et al., 2004). Sn propagation is not observed at the northwestern part of Iraq where Neogene and Quaternary volcanism exist.

These previous seismic studies indicate that lithospheric structure in the northern Arabian Platform is variable, but strongly correlated with tectonics. In this study we report crustal structure for two sites in Iraq from the joint inversion of P-wave receiver functions and surface wave group velocities. Results provide new constraints in structure of the northern Arabian Platform.

Data and Method

Receiver functions (RF's) isolate the response of near vertically propagating waves to seismic velocity discontinuities underneath a broadband seismic station [Langston 1977; Owens et al., 1984; Cassidy and Ellis, 1993]. Teleseismic P-waves RF's emphasize P-wave to S-wave conversions and are widely analyzed for crustal and upper mantle discontinuities. The P-to-S converted waves are isolated by deconvolving the vertical component from the radial to eliminate the source and the instrument response effects from the waveforms.

Two temporary broadband stations were deployed in Baghdad (BHD) and Mosul (MSL) in early 2005. The stations were equipped with Guralp CMG-3ESPD digital broadband seismometer. Unfortunately the data was noisy due to location of sites near major cities. Recording was intermittent reflecting of the difficult conditions in Iraq. However, we managed to pick a few large teleseismic events that could be used for RF analysis. In this study we employed the iterative time domain method [Ligorria and Ammon, 1999] to isolate the crustal response. In order to reduce the noise and improve the signal coherence we used a Gaussian filter with the bandwidth of 1.5 (~ 1 Hz). After eliminating the noisy events we stacked 7 individual RF's for MSL and 2 for BHD. Figure 2 shows a map of the event locations along with the individual and stacked RF's. The RF stacks were analyzed by themselves and in a joint inversion with surface wave group velocities.

First, we estimated the crustal thickness for both stations using the H-k stacking technique of Zhu and Kanamori [2000], where H is the Moho depth and k is the V_P/V_S ratio, related to Poisson's Ratio. This technique uses the amplitudes of receiver functions at the predicted arrival times of the crustal multiples by different crustal thickness H and V_P/V_S ratios. The best estimates of crustal thickness and V_P/V_S ratio are found when the three phases, i.e. Ps, PpPs, PpSs+PsPs, are stacked coherently. However, there are limitations and cases where this technique may fail, e.g., interference of crustal reverberated phase [Cassidy, 1992; Ammon et al., 1990]. We applied the technique over broad ranges of crustal thickness (25-60 km) and V_P/V_S (1.5-2.3). We observed a failure of this method at station BHD. It might be related to the thick sedimentary layer causing the multiple reverberations and interfering with the Moho converted phases. We were able to estimate the crustal thickness at MSL as shown in Figure 3. The Moho depth at station MSL is 38.9 ± 5.9 km and Vp/Vs is 1.90 ± 0.31.

Crustal RF's are primarily sensitive to the depth of velocity contrasts and have poor sensitivity to absolute velocities. Surface waves are primarily sensitive to depth averages of the S-wave velocity structure with poor sensitivity to velocity discontinuities. Julia et al. (2000, 2003) recently developed a method for estimating structure from the

joint inversion of RF's and surface wave group velocity dispersion curves. This method exploits the independent sensitivity of each data type to result in more reliable models. The non-uniqueness of each individual dataset can be reduced by combining surface waves with RF [Julia et al., 2000]. Using broadband data from the Eastern Turkey Seismic Experiment (ETSE), Gök et al., 2006 showed that shear wave velocities can be overestimated up to 0.5 km/s (> 10%) if only receiver function modeling is used. More reliable results for crustal velocity models are expected from the joint inversion of RF's and surface wave group velocity dispersion. Rayleigh waves and RFs are both sensitive to the vertically polarized S wave velocities. In this study we choose to use Rayleigh wave dispersion curves to be jointly inverted with receiver functions for two reasons. First, Gök et al., (2006) showed that the uncertainty of the models with Rayleigh waves and RF's are always smaller than Love waves and RF's. Second, when we include Love waves we were not able to fit Rayleigh+Love+RF simultaneously. This can be related to transverse anisotropy or Love waves having higher errors for continental-scale surface wave tomography. A recent study by Tkalcic et al. (2006) found that structure of the mantle lithosphere, including transverse isotropy, can be estimated from joint analysis of broadband (7-100 s) Love and Rayleigh wave dispersion.

Rayleigh wave dispersion curves for the station locations were extracted from tomographic images of group velocities in the band 7-100 seconds [Pasyanos, 2005]. The system of equations relating the observed RF and dispersion data to depth varying (plane-layered) shear velocity structure is inverted using the partial derivative matrices in damped least square sense. The models were parameterized with a series of layers, 2 km thick from 0-10 km and 3 km thick below. The inversion method uses an influence parameter (p) to adjust the relative weight of RF and dispersion data in the inversion. If p=0 the inversion is only for receiver function and p=1 is only for surface waves. We performed inversions using only Rayleigh waves and receiver functions at the range of p between 0 and 1 (0.3, 0.5 and 0.7). Generally, RF inversions are known to be non-unique and dependent on the starting model (Ammon et al., 1990). The dispersion data stabilizes the inversions. We also performed a test to find the optimum damping parameter between 0.3 and 0.8, and a value of 0.6 was chosen.

Results and Discussion

RF stacks, Rayleigh wave group velocity dispersion and the resulting models for two joint inversions at MSL and BHD are shown in Figures 4 and 5, respectively. The observed and predicted RF's at MSL and BHD are shown in Figure 4a and 5a, respectively. The observed (with 2σ uncertainties) and predicted Rayleigh wave group velocities at MSL and BHD are shown in Figures 4b and 5b, respectively. Figures 4c and 5c show the starting and resulting velocity models for MSL and BHD, respectively. For each site we used different starting models. Figures 4c and 5c show the resulting models using two very different starting models. One is a homogeneous earth model (where V_S= 4 km/s down to 110 km shown in dotted blue) and the other is an average continental crust model (shown in dotted red). There are no significant differences seen between the fits to the data for the two different input models. We tried other starting models and they too converged to the same final models. These test show the robustness of the solution.

The data available at station BHD was limited, only two individual RF's were judged appropriate for modeling. Note that the individual RF's for BHD (Figure 2) are very consistent except for the energy arriving at about 16 seconds. We tried to invert each individual BHD RF, thinking that the different ray parameters for each event could bias the modeling. However, we obtained similar fits for each inversion as those obtained from the inversion of the stacked RF. We concluded that the individual RF's are consistent with the stack and we preferred to use the stacked receiver functions (Figure 3).

At station MSL, in the northernmost part of Iraq, the joint receiver function and Rayleigh wave inversion resulted in a crustal thickness of about 39 km with average shear velocities of 3.1 km/s. Low velocities near the surface are interpreted as sedimentary layers with a thickness of 2 km. The uppermost mantle at MSL has velocities of 4.4-4.5 km/s. The Moho is not a sharp discontinuity in our model and is

apparently spread across 2 layers. This is consistent with the absence of a strong P_{SMoho} phase on the RF stack. The crustal thickness obtained from the joint inversion is very similar to what we obtained with H-k stacking technique (38.9 km, shown in Figure 3). The comparison between the observed and predicted receiver functions and surface wave dispersion curve is quite good (Figure 4). This estimate of crustal structure is very similar to one of the ETSE stations, MRDN [Gök et al., 2006], located south of the Bitlis suture on the Arabian Platform in the southernmost part of Turkey (crustal thickness of 38 km, Figure 4,c black line). The mid-crust at MSL reveals constant velocities in the range 15-38 km consistent with station MRDN.

At station BHD we infer a crustal thickness of 43 km with a 7 km thick layer of sediments (Figure 5). Uppermost mantle velocities are 4.4-4.5 km/s, consistent with those at station MSL. Low near surface velocities are required to fit the lower short-period (7-15 s) Rayleigh wave group velocities. Similar to MSL, the inversion results are not strongly sensitive to the starting model as indicated by the inversion results for two different models in Figure 5. We infer a larger velocity increase across the Moho for station BHD, consistent with the strong P_{SMoho} phase at about 4 seconds (Figure 5a). The mid- to lower crustal velocities are broadly consistent between stations MSL and BHD, with average values of about 3.6 km/s. The inferred crustal structure at station BHD can be compared with a recent study [Pasyanos et al., 2006] at station KBD (Kabd) in Kuwait, also located on a thick layer of Mesopotamian foredeep sediments. The crustal thickness at KBD is 45 km and sedimentary layer is 8 km.

Inversion of RF and Rayleigh wave dispersion data for two stations in Iraq reveals new constraints on the crustal structure of the northern Arabian Platform. The results are summarized in Figure 6. Also shown in Figures are results for two stations located on the Arabian Platform: MRDN in southeastern Turkey and KBD in Kuwait. Interestingly the crystalline crustal thickness, i.e. crustal thickness minus sediment thickness, at these stations is remarkably similar (about 36 km). Similarly, the average velocities of the crystalline crust (about 3.6 km/s) are consistent between these stations. This suggests

that the crustal structure of the Arabian Platform may have been largely uniform before subsidence and emplacement of the sedimentary structure.

Conclusion

Teleseismic and regional data from the newly available seismic stations, MSL and BHD, provided a unique opportunity to estimate the crustal velocity structure in the northern part of Arabian plate, Iraq. In spite of the fact that the data were limited, we were able to infer the crustal velocity structure. The joint inversion of stacked receiver functions and Rayleigh wave dispersion measurements were tested for their sensitivity to the starting models. We obtained very consistent velocity models down to about 100 km, indicating that the joint inversion is quite robust. The shear velocity structure, crustal thickness and the sedimentary layer depths are in good agreement with that observed at nearby stations in the northern Arabian Platform.

Our results show that the crustal thicknesses are 39km at station MSL and 43 km at BHD. The sedimentary thickness is about 3km at station MSL and 8km at BHD. The deeper sedimentary layer at BHD can be expected to amplify earthquake ground motions. The sedimentary thickness appears to comply well with the existing models (e.g. Laske et al., 1997). In fact the main difference between our results at MSL and BHD and those at nearby stations MRDN (southern Turkey) and KBD (Kuwait) are in the sedimentary structures. The crystalline crustal structure is very consistent between these stations, separated by over 1000 km. However, these sites are located at about the distance from the MZT. It would be valuable to sample the crustal thickness perpendicular to the MZT to see if crustal thicknening has occurred in the Arabian Platform away from the MZT. Recent results from Paul et al (2006) along a crustal transect across the Zagros Mountains from the Gulf to the Iranian interior indicate that crustal thickness is about 45 km in the Arabian Platform and thickens significantly at the MZT. So it is possible that the entire northern Arabian Platform is composed of uniform crustal structures with only the sedimentary structure varying. Future seismic investigations based on new broadband data will be needed to bring light to this issue.

Acknowledgements

We like to thank Charles Ammon for making his time-domain receiver function code available and Jordi Julia for sharing his joint inversion codes. This work was performed under the auspices of the U.S. Department of Energy by University of California, Lawrence Livermore National Laboratory under Contract W-7405-Eng-48. This is LLNL contribution UCRL-TR-??????.

References

Adams, R.D. and Barazangi, M., (1984). Seismotectonics and seismology in the Arab region: a brief summary and future plans. Bull. Seismol. Soc. Am., 74: 1011-1030.

Al-Heety, E.A.M., (2002) Crustal structure of the northern Arabian platform inferred using spectral ratio method, Journal of Geodynamics, Vol. 34, pp. 63–75

Al-Lazki, A., Sandvol, E., Seber, D., Barazangi, M., Mohammad, R., and Turkelli, N. (2003). Pn tomographic imaging of mantle lid velocity and anisotropy at the junction of the Arabian, Eurasian, and African plates, *Geophys. Res. Lett.*, 30, 8043-8046.

Al-Lazki, A., E. Sandvol, D. Seber, M. Barazangi, N. Turkelli, and R. Mohammed (2004). On tomographic imaging of mantle lid velocity and anisotropy at the junction of the Arabian Eurasian and African plates, Geophys. J. Int., 158, 1024-1040.

Al-Naqib, K.M. (1967) Geology of the southern area of Kirkuk Liwa, Tech. Publ., Iraq Petrol. Co. Ltd., 50P.

Alsinawi, S (2002). Middle East Seismological Forum and Its Role in Research Promotion in the Region, International Workshop on Seismic Analysis and Earthquake Hazard Assessment in the Mediterranean Region, Antakya, Turkey.

Alsinawi, S. A. and H. A. A. Ghalib (1975). Historical seismicity of Iraq, *Bull. Seis. Soc. Am.* 65,541-547.

Alsinawi, S. A. and I. Banno (1976). The first microearthquake recording in Iraq, *Tectonophysics* 36, T1-T6.

Alsinawi, S. A. and H. A1-Shukri (1979). Microseismicity of the Badra area--Iraq, *Tectonophysics* 60, 289-292.

Ambraseys, N. N. and C. P. Melville (1982). *A History of Persian Earthquakes,* Cambridge University Press, London, England, 219 pp.

Ammon, C.J., Randall, G.E. & Zandt, G. (1990). On the non-uniqueness of receiver function inversions, *J. Geophys. Res.*, 95**,** 15303-15318.

Berberian, M. (1976). Contribution to the seismotectonics of Iran, part II, Geol. Survey of Iran, Report No. 39, 516 pp.

Buday**,** T., (1980) Regional Geology of Iraq, Vol.1 Stratigraphy, I.I.M. Kassab and S. Z. Jassim (Edts.), D. G. Geol. Surv. Min. Invest., Publications, Baghdad, 445 P.

Ditmar, et.al. (1971) Geological conditions and hydrocarbon prospects of the Republic of Iraq, North-central, contract no. 50998, SOM library (unpublished).

Dunnington, H.V. (1958) Generation, migration, accumulation and dissipation of oil in Northern Iraq, (Habitite of oil) 1194-1251.

Engdahl, R.E., van der Hilst, R., and Buland, R.P., (1998), Global teleseismic earthquake relocation with improved travel times and procedures for depth determination. Bull. Seismol. Soc. Am. 88, 722–743.

Engdahl, R.E., Jackson, J.A., Myers S.C., Bergman E.A. and Priestley K., (2006) Relocation and assessment of seismicity in the Iran region, in press Geophys. J. Int.

Gök R., M. Pasyanos and E. Zor, (2006) Lithospheric Structure of the Continent-Continent Collision Zone: Eastern Turkey, in press Geophys. J. Int. .

Julià, J., Ammon, C.J., Herrmann, R.B. & Correig, A.M., 2000. Joint inversion of receiver functions and surface-wave dispersion observations, *Geophys, J. Int.*, 143, 99-112.

Julià, J., Ammon, C.J. & Herrmann, R.B., 2003. Lithospheric structure of the Arabian Shield from the joint inversion of receiver functions and surface-wave group velocities, *Tectonophysics*, 371, 1-21.

Kadinsky-Cade, K. and M. Barazangi (1982). Seismotectonics of southern Iran: the Oman line, *Tectonics* 1,389-412.

Kassler, P. (1973). The structural and geomorphic evolution of the Persian Gulf, in *The Persian Gulf, B.* Purser, Editor, Springer-Verlag, New York, 11-32.

Langston, C.A. (1979). Structure under Mount Rainer, Washington, inferred from teleseismic body waves, *J. Geophys. Res.*, 84, 4749-4762.

Ligorría, J.P. & Ammon, C.J. (1999). Iterative deconvolution and receiver function estimation, *Bull. Seism. Soc. Am.*, **89**, 1395-1400.

Maggi, A. and K. Priestley (2005). Surface waveform tomography of the Turkish-Iranian Plateau, *Geophys. J. Int*., 160, 1068-1080.

Nowroozi, A. A. (1972). Focal mechanism of earthquakes in Persia, Turkey, West Pakistan, and Afghanistan, and plate tectonics of the Middle East, *Bull. Seism. Soc. Am.* 62,823-850.

Owens, T.J., Zandt, G. & Taylor, S.R. (1984). Seismic evidence for an ancient rift beneath the Cumberland Plateau, Tennessee: A detailed analysis of broadband teleseismic P waveforms, *J. Geophys. Res.,* 89, 7783-7795.

Pasyanos M. E. (2005), A variable resolution surface wave dispersion study of Eurasia, North Africa, and surrounding regions, J. Geophys. Res., 110, B12301, doi:10.1029/2005JB003749.

Pasyanos, M. E., and W. R. Walter (2002), Crust and upper-mantle structure of North Africa, Europe, and the Middle East from inversion of surface waves, *Geophys. J. Int.*, *149*, 463–481.

Pasyanos, M. E., W. R. Walter, and M. P. Flanagan (2003), A lithospheric study of eastern Asia using surface wave dispersion, *Eos Trans. AGU*, *84*(46), Fall Meet. Suppl., Abstract S32E-08.

Pasyanos M.E., H Tkalčić, R Gök, A.J. Rodgers, and A. Al-Enezi, Seismic structure in Kuwait, in preparation.

Paul, A., A. Kaviani, D. Hatzfeld, J. Vergne, M. Mokhtari (2006). Seismological evidence for crustal-scale thrusting in the Zagros mountain belt (Iran), Geophys. J. Int., 166, 227-237

Ritzwoller, M. H., A. L. Levshin, (1998). Eurasian surface wave tomography: Group velocities, J. Geophys. Res., 103(B3), 4839-4878, 10.1029/97JB02622.

Seber, D., Marisa Vallve, Eric Sandvol, David Steer, and Muawia Barazangi, (1997), Geographic Information Systems (GIS) in earth sciences: An application to the Middle East region, GSA Today.

Stocklin, J. (1968). Structural history and tectonics of Iran: a review, *Bull. Am. Assoc.Petrol. Geol.* 52, 1229-1258.

Zhu, L., and H. Kanamori (2000), Moho depth variation in southern California from teleseismic receiver functions, *J. Geophys. Res.*, *105*, 2969–2980.

Figure Captions

Figure 1 Tectonic setting and sedimentary thickness map of region is shown as contour lines. BHD is located near thicker sediments whereas MSL is at the transition from thinner to thicker sediments with respect to Laske et al., 1997 model.

Figure 2 Teleseimic receiver functions obtained with iterative deconvolution technique (gray) and the stacked ones (black) for each station. The two events at station BHD are from completely different locations yet they are quite similar. The event locations are shown as circles on the global map and the triangle is MSL/BHD (upper right)

Figure 3 The receiver function h-k stacking at MSL station. Vp/Vs ratio is higher then the average (1.73). Standard deviations are obtained with boot-strapping technique. Individual receiver functions are shown with theoretical onset of multiples (red lines with phase names) at h=38.9 km and Vp/Vs=1.9

Figure 4 Joint inversion result for station MSL. Black line is observed/stacked receiver function, black dotes are Rayleigh waves group velocities with error bars. Red and blue solid lines are inversion results of corresponding input model. Black line on panel c is the inversion solution of station MRDN in southeastern Turkey.

Figure 5 Joint inversion result for station BHD. Black line is the observed/stacked receiver function, black dotes are Rayleigh waves group velocities with error bars. Red and blue solid lines are inversion results of corresponding input model

Figure 6 The crustal and sedimentary thickness are given together with Laske et al., 1997 sedimentary thickness model and the results from previous studies at MRDN (ETSE station) and KBD (Kuwait). BHD and KBD have similar Moho depth and sedimentary layer. MSL and MRDN are thinner.

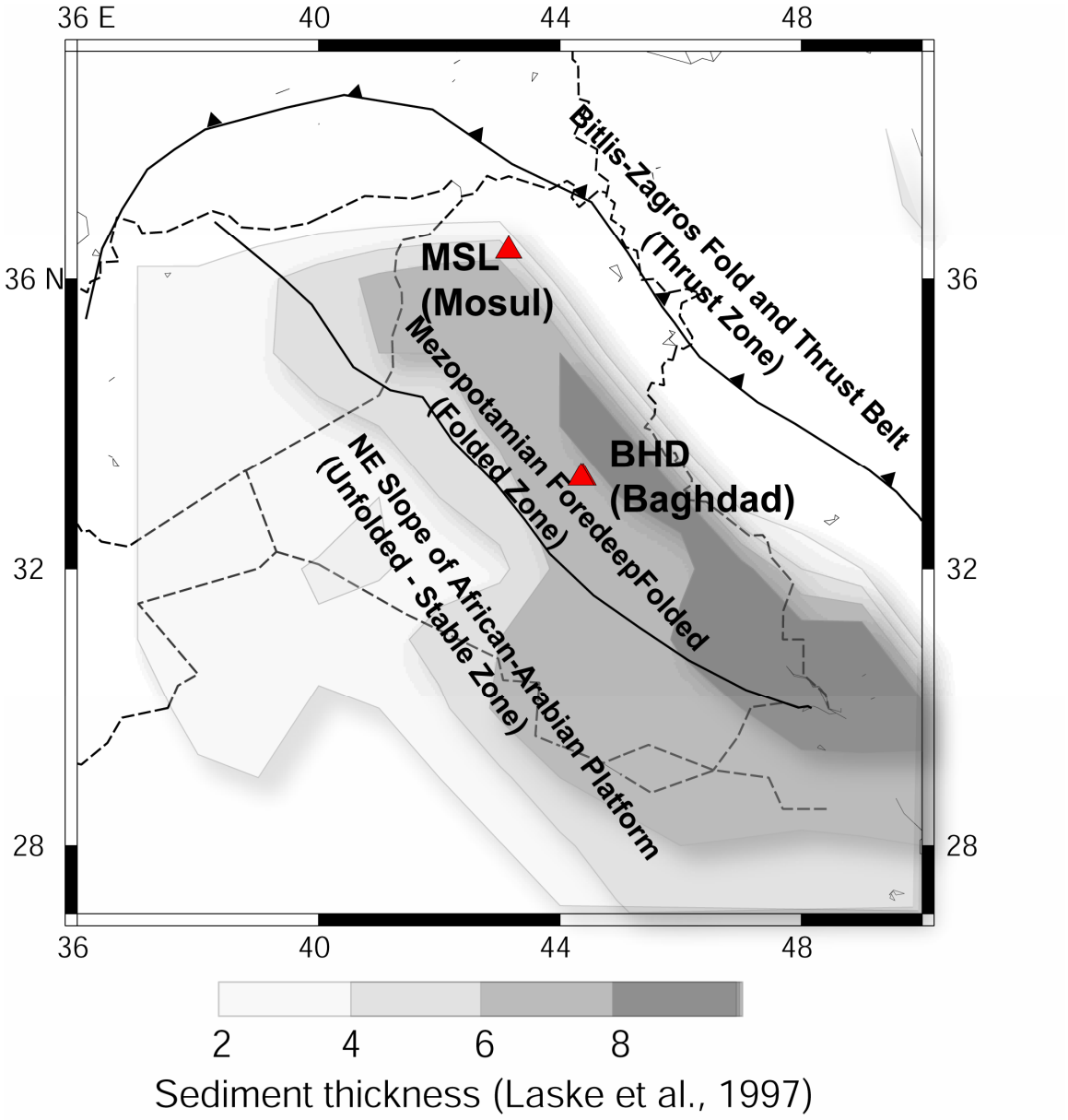
36 E
40
44
48
36 N
36
32
28
36
40
44
48
MSL
(Mosul)
BHD
(Baghdad)
Bitlis-Zagros Fold and Thrust Belt
(Thrust Zone)
Mezopotamian ForedeepFolded
(Folded Zone)
NE Slope of African-Arabian Platform
(Unfolded - Stable Zone)
2
4
6
8
Sediment thickness (Laske et al., 1997)

Figure 1

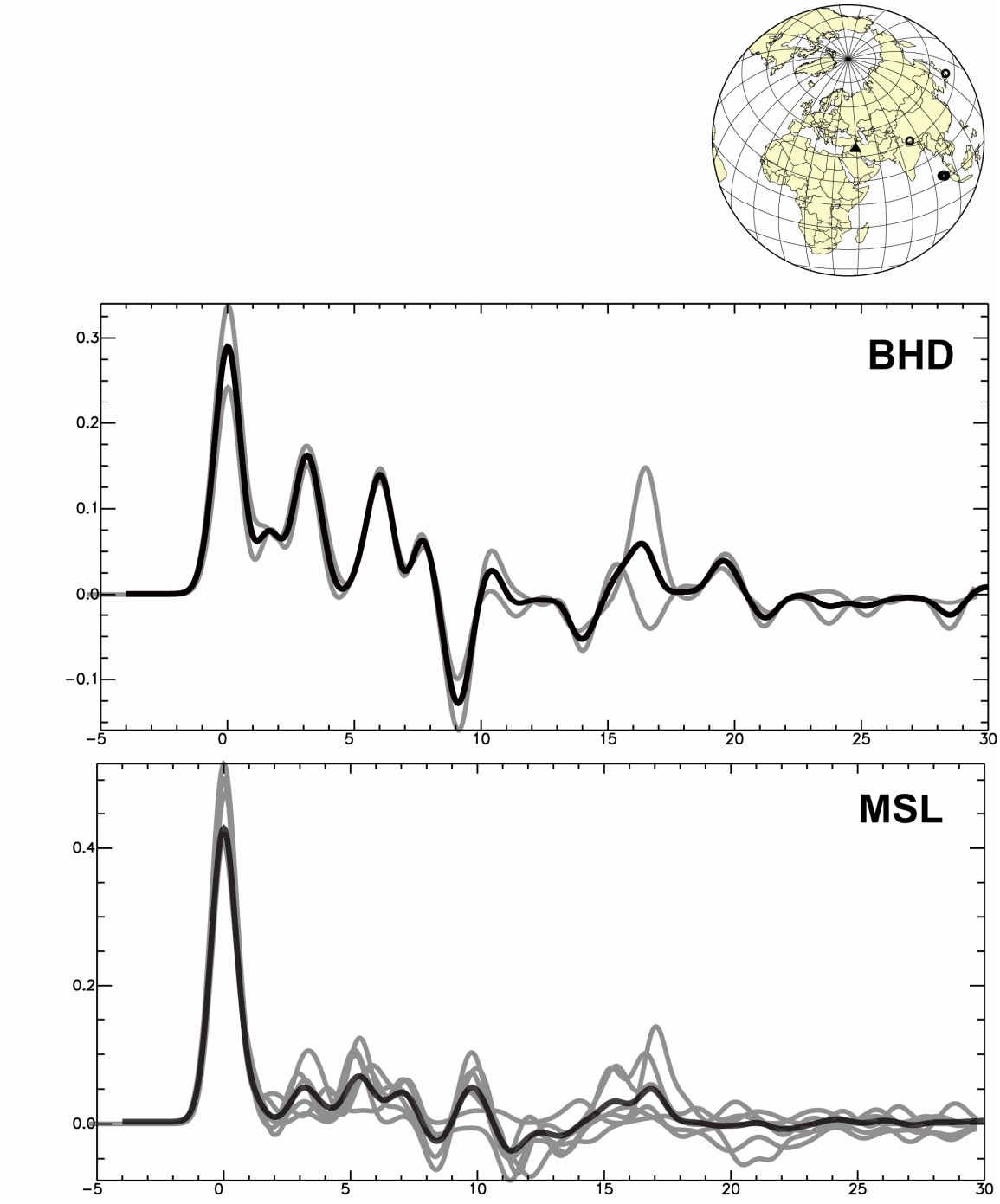

Figure 2

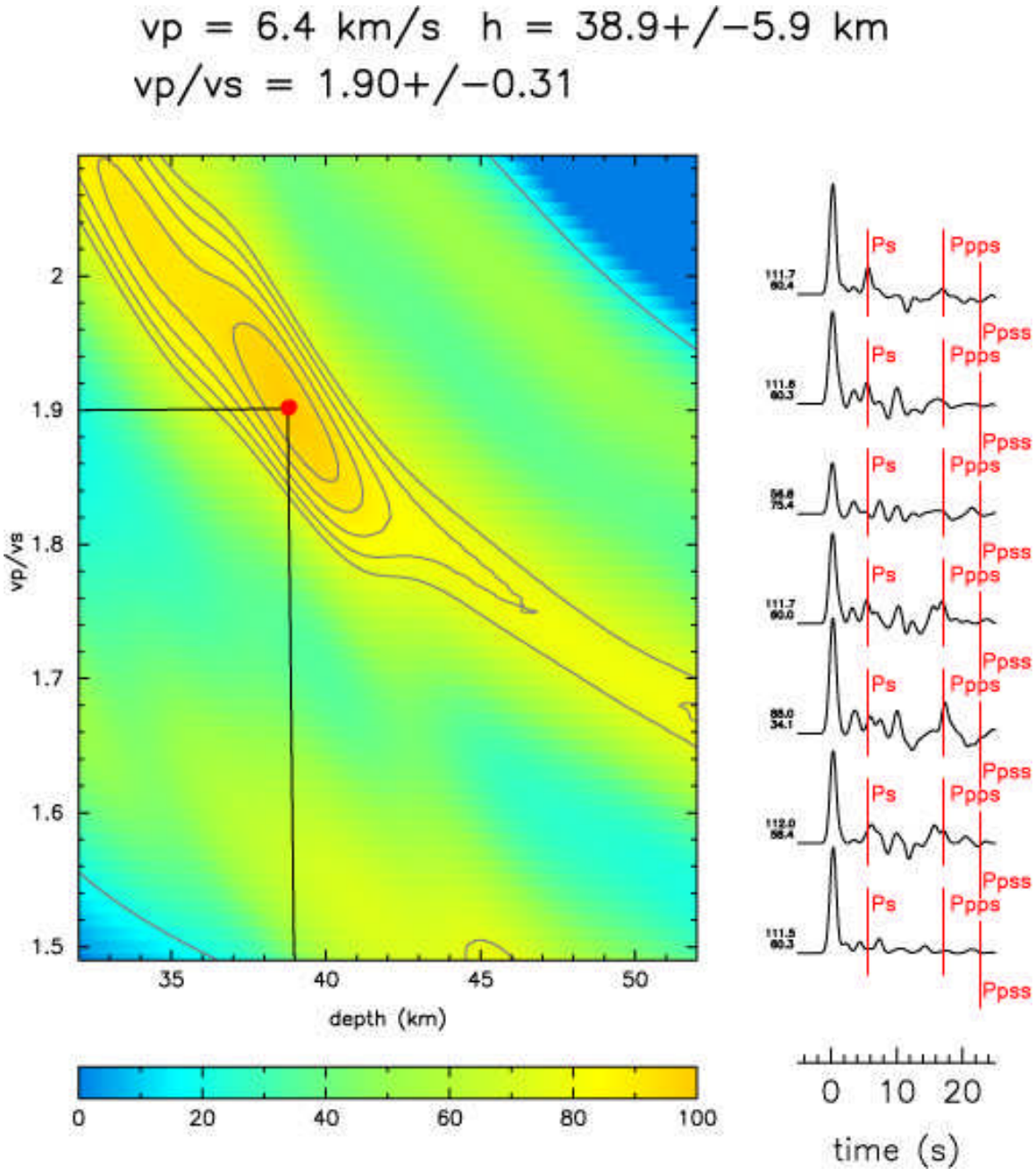
vp = 6.4 km/s h = 38.9+/−5.9 km
vp/vs = 1.90+/−0.31
vp/vs
2
1.9
1.8
1.7
1.6
1.5
35
40
45
50
depth (km)
0
20
40
60
80
100
Ps
Pps
Pss
0
10
20
time (s)

Figure 3

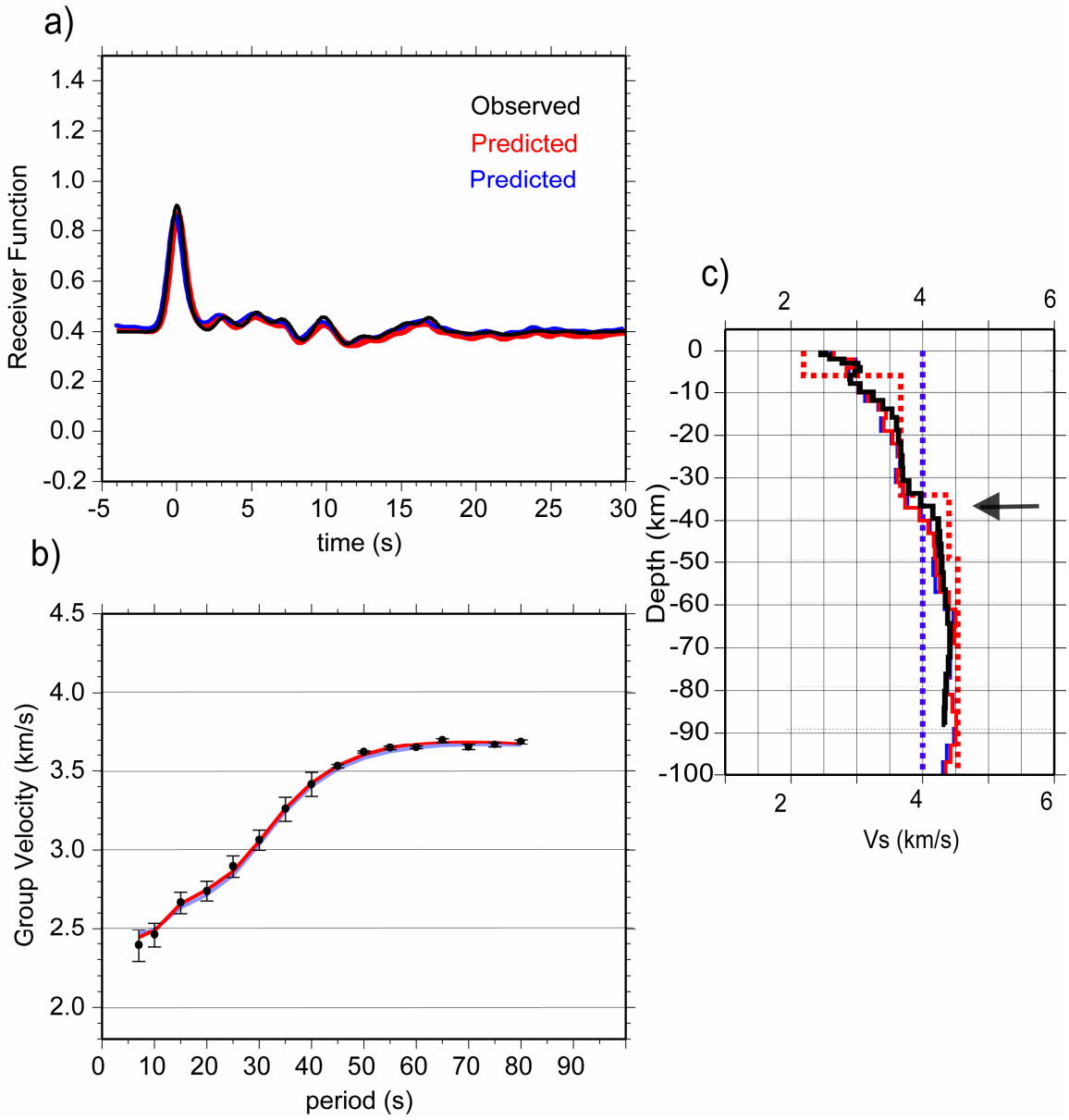
a)
Observed
Predicted
Predicted
Receiver Function
time (s)
b)
Group Velocity (km/s)
period (s)
c)
Depth (km)
Vs (km/s)

Figure 4

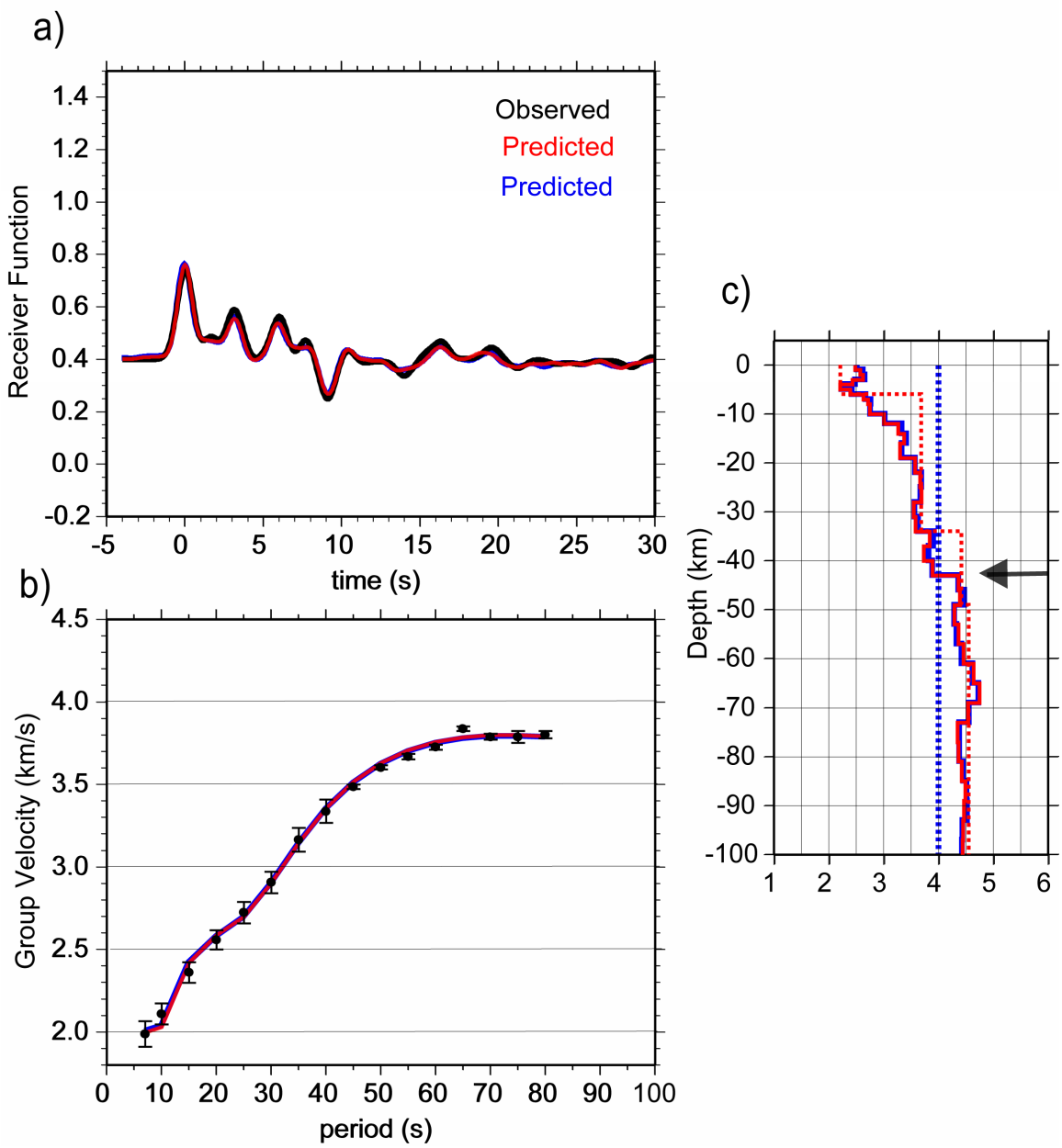
a)
Observed
Predicted
Predicted
Receiver Function
time (s)
b)
Group Velocity (km/s)
period (s)
c)
Depth (km)

Figure 5

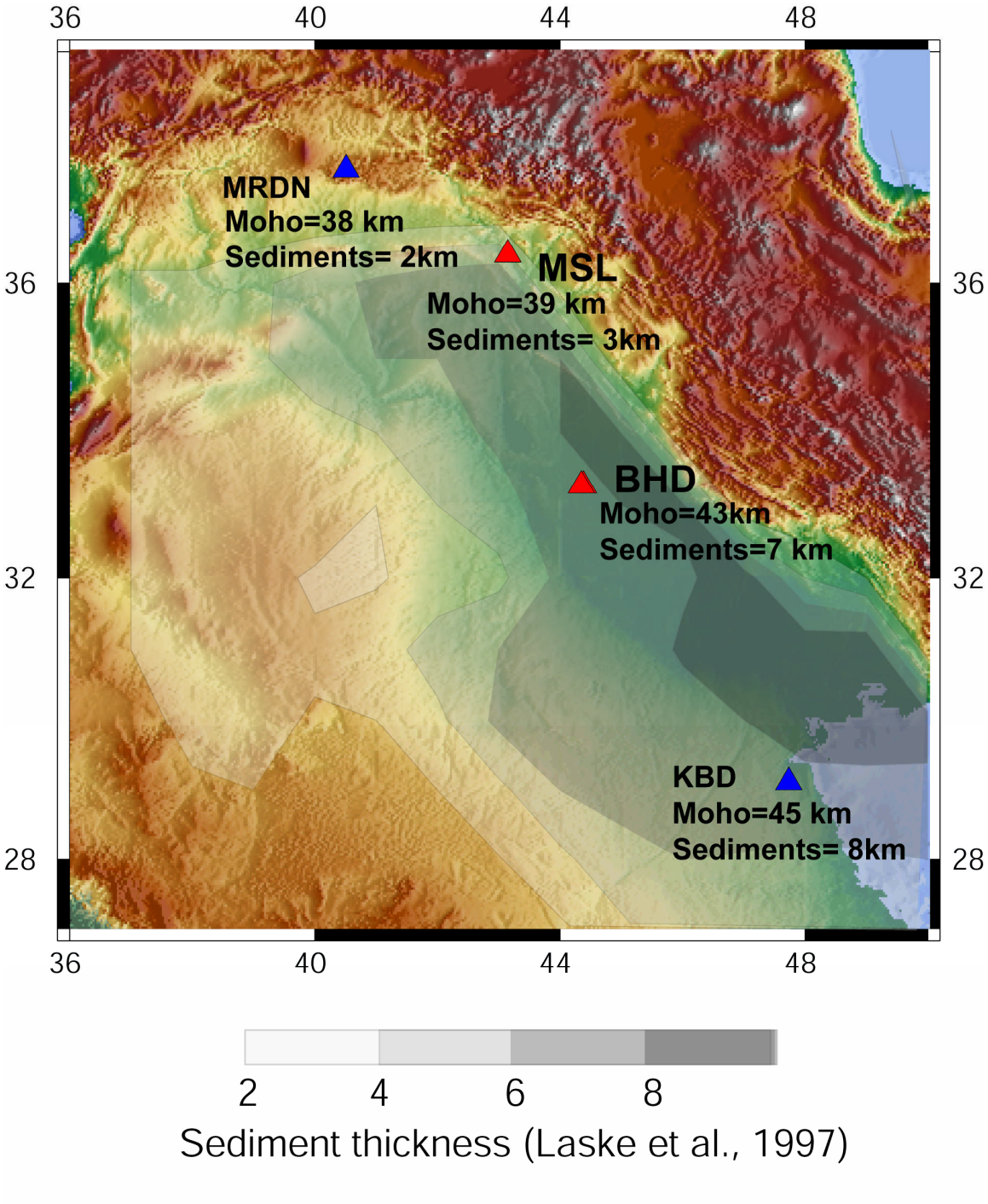
36
40
44
48
36
32
28
MRDN
Moho=38 km
Sediments= 2km
MSL
Moho=39 km
Sediments= 3km
BHD
Moho=43km
Sediments=7 km
KBD
Moho=45 km
Sediments= 8km
2
4
6
8
Sediment thickness (Laske et al., 1997)

Figure 6